Tellus (1988), *40A*, 50–60

Transient climatic response to increasing CO_2 concentration: some dynamical scenarios

By C. NICOLIS, *Institut d'Aéronomie Spatiale de Belgique, 3, Avenue Circulaire, 1180 Bruxelles, Belgium*

(Manuscript received January 2; in final form March 17, 1987)

ABSTRACT

The global surface temperature record of the last 130 years displays a stage of systematic increase on which is superimposed a small-scale variability, followed by a stage of marked slowing down. At first sight, this appears to be surprising, in view of the ongoing increase of CO_2 concentration in the atmosphere. In this work, the mechanisms that enable a dynamical system to produce such a peculiar response to an increasing control parameter are studied. The main ideas are illustrated, successively, on a linearized energy balance model subject to white or red noise, on nonlinear energy balance models admitting several stable solutions, and on a simple thermal convection model giving rise to nonperiodic (chaotic) solutions. It is shown that the action of stochastic perturbations (especially those having a relatively long correlation time), the sudden switching in the vicinity of a point of marginal stability, or finally chaotic dynamics, give rise to responses that match the temperature record. It is suggested that the variance of climatic observables is much more sensitive to the increase of a control parameter compared to the mean.

1. Introduction

The climatic impact of the CO_2 increase in the atmosphere has attracted considerable interest in recent years. Models of varying complexity, from simple energy-balance models to detailed general circulation ones have been analyzed, and although their predictions differ in many respects, they seem to agree on one crucial point: the enhancement of global surface temperature by several degrees as a result of CO_2 doubling (see for instance D.O.E. (1985) and references therein).

Now, the inspection of the currently available record of global temperature trends suggests that the thermal response is much subtler than a steady increase in temperature. Specifically, despite the numerous uncertainties arising from estimates of global variables, it appears that the global surface temperature record of the last 130 years is rather "wiggly", regardless of the resolution adopted, and that it displays a rather marked plateau in the last few decades or so which is especially apparent in the northern hemisphere data (Jones et al., 1986).

A number of arguments have been advanced to explain this apparent discrepancy. Let us quote for instance, the possibility that natural fluctuations or climatic cycles may mask the predicted temperature trend; the opposing effect of anthropogenic aerosols accompanying CO_2 emissions from fossil fuel combustion; or the thermal storage ability of the world's oceans (Broecker, 1975; Schneider and Mass, 1975; Bryson and Dittberner, 1976; Hoffert et al., 1980). Nevertheless, the legitimate question arose whether current climatic models are not overestimating the sensitivity of climate to a doubled CO_2 concentration (Newell and Dopplick, 1979; Idso, 1982).

Our purpose in the present work is to identify the prerequisites that must be satisfied by a system in order to produce a response to an increasing control parameter similar to the observed surface temperature trend: a period of systematic increase (on which is superimposed a small scale variability) followed by a slowing down or even by a plateau. The motivation for raising this question is in the fact that physical systems, regardless of their complexity, present

only a limited number of qualitatively different dynamical behaviors. The latter rest on some very general features of the underlying dynamics and are largely independent of the details of the individual processes. We hope, therefore, that this study will shed some light on the mechanisms presiding over the observed thermal response of the climatic system to the ongoing CO_2 increase.

The paper is organized as follows. In Section 2, we consider a linear system subject to both a random noise and a systematic increase of a control parameter and show that despite the systematic increase of the mean, the stochastic response matches certain features of the record in an appropriate range of values of the variance and correlation time of the noise. In Section 3, we consider a nonlinear energy balance model giving rise to multiple steady states and evaluate its response to a sudden or to a gradual CO_2 increase. We show that in the absence of fluctuations, only the response to the (unrealistic) stepwise increase matches the general features of the record. This conclusion is extended, in Section 4, to any model involving a jump to a new steady state arising beyond a limit-point bifurcation. The situation appears to be different in systems involving limit cycles or chaotic dynamics, considered in Section 5. We show that under certain conditions, such systems can produce a response which is qualitatively similar to the observed temperature trend, even in the absence of random noise. The main conclusions are finally drawn in Section 6.

2. Linear response theory

The general form of the energy balance equation for the globally averaged temperature T reads:

$$C\frac{dT}{dt} = Q(1 - a(T)) - (\text{infrared cooling terms}), \tag{1}$$

where Q is the solar constant divided by 4, C the heat capacity and a the albedo. In this section, we assume that the range of variation of surface temperature around a reference state T_0 (corresponding, for instance, to pre-industrial conditions), induced by the CO_2 increase, is small. This will allow us to *linearize* eq. (1) around T_0. In writing the explicit form of the energy budget, we use a result of radiative convective models, according to which a systematic CO_2 increase will show up as an additive contribution of the form $\tilde{K} \ln c/c_0$, where c is the CO_2 concentration at a given time, c_0 its value at the reference state and $\tilde{K}$ a constant (Augustsson and Ramanathan, 1977). Detailed studies suggest that c/c_0 varies exponentially (see for instance Keeling and Bacastow, 1977); hence the CO_2 contribution in the radiation budget will be reflected by an additive, linearly increasing term in time. In addition, to account for the natural variability of climate which, as mentioned in the Introduction, is invoked to explain qualitatively the slowing down of the temperature increase observed in the record, we introduce a stochastic forcing term. The linealized energy balance equation thus takes the form:

$$\frac{dx}{dt} = -\lambda x + \frac{\tilde{K}}{C}\varepsilon t + \frac{1}{C}g(x)F(t). \tag{2}$$

Here $x = T - T_0$, ε is the rate of CO_2 increase, λ is the inverse relaxation time, $F(t)$ a noise process, and $g(x)$ a term expressing the coupling between the dynamics and the fluctuations. $F(t)$ will successively be taken to be Gaussian white noise of variance equal to q^2, and red noise. Additive fluctuations ($g = 1$) and multiplicative ones ($g = -\lambda x$) will also be considered.

2.1. *Case of Gaussian white noise*

Eq. (2) is equivalent to a Fokker-Planck equation for the probability density $P(x, t)$ (Nicolis and Nicolis, 1981).

$$\frac{\partial P}{\partial t} = -\frac{\partial}{\partial x}\left(-\lambda x + \frac{\tilde{K}}{C}\varepsilon t\right)P + \frac{q^2}{2C^2}\frac{\partial^2}{\partial x^2}(g^2 P), \tag{3}$$

wherein the Ito interpretation has been adopted (Gardiner, 1983). Multiplying both sides successively by x and x^2 and integrating over x we obtain:

$$\frac{d\bar{x}}{dt} = -\lambda\bar{x} + \frac{\tilde{K}}{C}\varepsilon t, \tag{4a}$$

$$\frac{d\overline{x^2}}{dt} = -2\lambda\overline{x^2} + \frac{2\tilde{K}}{C}\varepsilon t\bar{x} + \frac{q^2}{C^2}\overline{g^2}, \tag{4b}$$

where the bar denotes averages taken with $P(x, t)$. Note that eq. (4a) is the (linearized)

globally averaged energy balance in the absence of fluctuations. It can be solved straightforwardly, and we obtain:

$$x = x_0 e^{-\lambda t} + \frac{\varepsilon \tilde{K}}{C\lambda}\left(t + \frac{e^{-\lambda t} - 1}{\lambda}\right), \tag{5}$$

where x_0 is the initial condition. We see that after a lapse time $t \geqslant \lambda^{-1}$, $\bar{x}$ is a linear function of t with a slope equal to $\varepsilon\tilde{K}/(\lambda C)$. Since λ itself is inversely proportional to C, this limiting regime is therefore *independent of the heat capacity*. In other words, the mean temperature follows passively the linear increase of CO_2, the only effect of the internal dynamics being to modulate the rate ε by a numerical factor, depending solely on the radiative parameters of the system.

Let us now turn to $\overline{x^2}$ or, more significantly, to the variance $\overline{\delta x^2} = \overline{x^2} - \bar{x}^2$. Multiplying (4a) by $\bar{x}$ and subtracting the result from (4b) we obtain:

$$\frac{d}{dt}\overline{\delta x^2} = -2\lambda\,\overline{\delta x^2} + \frac{q^2}{C^2}\overline{g^2}. \tag{6}$$

More specifically: (i) For additive fluctuations, $g = 1$, the steady-state solution of eq. (6) is

$$\overline{\delta x_s^2} = \frac{q^2}{2\lambda C^2}. \tag{7}$$

In other words, in this model the temperature variability is independent of the CO_2 increase. (ii) For multiplicative fluctuations, $g = -\lambda x$, eq. (6) becomes

$$\frac{d}{dt}\overline{\delta x^2} = \left(-2\lambda + \frac{q^2}{C^2}\lambda^2\right)\overline{\delta x^2} + \frac{q^2}{C^2}\lambda^2\,\overline{x^2}. \tag{8a}$$

This equation predicts an enhancement of the lifetime of the fluctuations relative to that of the mean. In addition, a stochastic instability (blow-up of fluctuations) is expected if $q^2 > 2C^2/\lambda$. Otherwise, the long-time solution is given by

$$\overline{\delta x^2} = \frac{1}{\left|\left(\frac{q}{C}\lambda\right)^2 - 2\lambda\right|}\,\frac{q^2\tilde{K}^2}{C^4}\varepsilon^2 t^2. \tag{8b}$$

In other words, the variance of the variable is now sensitive to the CO_2 increase. This latter property is in accordance with the increased variability observed in the record (Angell and Korshover, 1977).

The extent to which the fluctuations will affect the observed record depends on their variance or, more precisely, on the ratio $q/(\lambda^{1/2}C)$. Notice that, since $\lambda \sim 1/C$, the heat capacity affects the variance by a factor of $C^{-1/2}$. A large heat capacity reflecting, for instance, the coupling between atmospheric dynamics and deep ocean circulation, tends thus to smear out the effectiveness of the fluctuations. Fig. 1 depicts the results of numerical solutions of the stochastic differential equation (2) in the additive noise case, carried out for $\varepsilon = 0.01$ year^{-1}, $\tilde{K}/C = 0.17$ year^{-1} and for different values of the parameter $q/(\lambda^{1/2}C)$. In each case, the parameters λ and C are taken from Hoffert and Flannery (1985) such that $\lambda^{-1} \sim 4$ year, (the characteristic radiative cooling rate of the mixed layer) and q^2/C^2 takes successively the values 6.9×10^{-5}, 2.8×10^{-4}, 6.9×10^{-3} year^{-1}, all of which are in agreement with the inequality $q/(\lambda^{1/2}C) < 1$. As we see from the figure, the systematic increase of CO_2 is reflected by the property that fluctuations toward positive values of x strongly dominate the negative ones. Still, in a given realization, one observes patterns reminiscent of the record. As expected, this deviation from the mean behavior is more pronounced for the largest value of q^2 (curve (c) in Fig. 1), for which, for instance, after a period of increase by about 0.4 K, the system slows down and saturates before a further increase to about 0.5 K is recorded. More significantly perhaps, even in the small variance case, there are episodes of increase by about 0.2 K followed by a plateau (curve (b) in Fig. 1). Notice however that in all cases, the

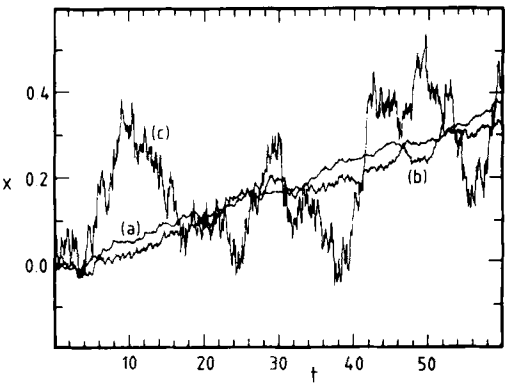

Fig. 1. Time evolution of the variable x obtained by numerical integration of eq. (2) with $g = 1$ and $F(t)$ a Gaussian white noise: curve (a) $q^2/C^2 = 6.9 \times 10^{-5}$; curve (b) $q^2/C^2 = 2.8 \times 10^{-4}$ and curve (c) $q^2/C^2 = 6.9 \times 10^{-3}$ year^{-1}.

variability is rather short-lived, a property that is to be attributed to the white noise character of the stochastic forcing.

2.2. Red noise

We next consider the case in which eq. (2) is forced by an additive Ornstein-Uhlenbeck noise $z(t)$. The evolution reduces now to the pair of equations

$$\frac{dx}{dt} = -\lambda x + \frac{\tilde{K}}{C}\varepsilon t + \frac{1}{C}z(t),$$
$$\frac{dz}{dt} = -\gamma z + F(t), \tag{9}$$

in which $F(t)$ denotes as before a Gaussian white noise of variance q^2 and γ is the inverse correlation time of the z-process. It is well-known that the pair (x, z) is a Markovian process described by the bivariate Fokker-Planck equation

$$\frac{\partial P}{\partial t} = -\frac{\partial}{\partial x}\left(-\lambda x + \frac{\tilde{K}}{C}\varepsilon t + \frac{1}{C}z\right)P - \frac{\partial}{\partial z}(-\gamma z)P + \frac{q^2}{C^2}\frac{\partial^2}{\partial z^2}P. \tag{10}$$

Owing to the linearity of the coefficients, the first and second moment equations can be again decoupled. Following the same procedure as in the derivation of eqs. (4), we obtain:

$$\frac{d\bar{x}}{dt} = -\lambda\bar{x} + \frac{\tilde{K}}{C}\varepsilon t + \frac{1}{C}\bar{z}, \tag{11a}$$

$$\frac{d\bar{z}}{dt} = -\gamma\bar{z}, \tag{11b}$$

$$\frac{d\overline{\delta x^2}}{dt} = -2\lambda\overline{\delta x^2} + \frac{2}{C}\overline{\delta x\,\delta z}, \tag{12a}$$

$$\frac{d\overline{\delta z^2}}{dt} = -2\gamma\overline{\delta z^2} + q^2, \tag{12b}$$

$$\frac{d\overline{\delta x\,\delta z}}{dt} = -(\gamma+\lambda)\overline{\delta x\,\delta z} + \frac{1}{C}\overline{\delta z^2}. \tag{12c}$$

After a lapse of time of the order of γ^{-1}, $\bar{z}$ becomes close to zero and $\bar{x}$ follows the same behavior as in eq. (5). As for the variances, they are again independent of the systematic increase of CO_2 and attain steady-state values given by

$$\overline{\delta x_s^2} = \frac{q^2}{2\lambda C^2}\frac{1}{\gamma(\gamma+\lambda)}, \quad \overline{\delta z_s^2} = \frac{q^2}{2\gamma},$$
$$\overline{\delta x_s\,\delta z_s} = \frac{1}{(\gamma+\lambda)}\frac{q^2}{2\gamma C}. \tag{13}$$

It follows from these equations, that for a given value of the variance q^2, the effectiveness of the fluctuations increases when γ decreases, that is to say when the correlation time of the red noise increases.

Fig. 2 reports the results of the numerical integration of the pair of eqs. (9) for the same values of λ, C, ε as in Fig. 1, for $q^2/C^2 = 2.8 \times 10^{-6}$, 6.9×10^{-5}, 2.8×10^{-4} year^{-3} and for $\gamma = 0.1$ year^{-1}. Certain differences from Fig. 1 are worth pointing out. First, the evolution is much smoother; second, an increasing stage followed by a slowing down is again observed, but this time it is more marked and extends over a longer period of time. This is clearly a "memory" effect due to the finite correlation time of the forcing. As a consequence of all these features, the evolution is closer to the observed record as compared to the white noise case.

3. An energy balance model involving multiple steady states

As long as the energy balance equation admits only one solution for given parameter values, the addition of higher order terms in eq. (1) will not sensibly modify the behavior obtained in Section 2. We now consider the next qualitatively different possibility, namely that the energy balance equation (1) admits several stable solution branches in the vicinity of the present day global

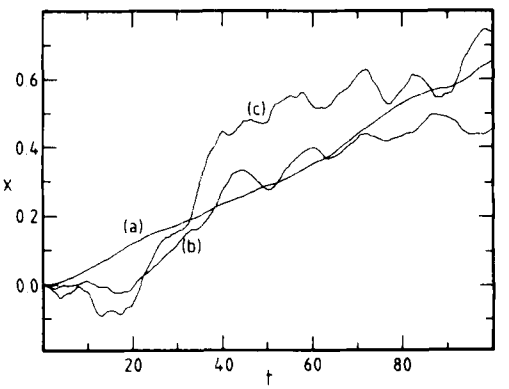

Fig. 2. As in Fig. 1, but with $F(t)$ an Ornstein-Uhlenbeck noise and $\gamma = 0.1$ year^{-1}; curve (a) $q^2/C^2 = 2.8 \times 10^{-6}$; curve (b) $q^2/C^2 = 6.9 \times 10^{-5}$ and curve (c) $q^2/C^2 = 2.8 \times 10^{-4}$ year^{-3}.

temperature. Although there is no direct experimental evidence for multiple steady states (or of the existence of a unique steady state for that matter), it is nevertheless instructive to explore this possibility, since it constitutes one of the typical modes of behavior of a complex system.

For simplicity, we shall adopt a parameterization of infrared cooling terms whereby these terms are expressed as a linear function of the deviation of T from a reference state T_0 to which a negative contribution K arising from CO_2 increase is added (see for instance Hoffert and Flannery, 1985). In most of the analysis, K will be linear in time, but for the moment it will merely be regarded as an additional parameter. In the absence of stochastic forcing, eq. (1) then becomes (we set $T = T_0 + x$):

$$C\frac{dx}{dt} = Q[1 - a(T_0 + x)] - (A + Bx - K),$$

$$K > 0. \tag{14}$$

The question that arises now is how to model the albedo as a function of temperature. In studies devoted to long-term variability, it is generally accepted that $a(T)$ can be represented as a step function or, better as a continuous function of T consisting of two plateaus (high for low $T(T < T_1)$, low for high $T(T > T_2)$) connected by a region of linear dependence. This gives rise quite naturally to multiple steady-state solutions, but for realistic parameter values, the additional stable solutions thus obtained are in general quite far from present day conditions. In this study, we keep the general idea of the albedo as a piecewise linear and continuous function of T, focus on a temperature range close to present day one, and replace the region of linear dependence by two linear regions with different slopes (Fig. 3). In justification of this Ansatz, we argue that if T increases by a few degrees compared to the reference value T_0, the eddy diffusivity D will be enhanced. Indeed, according to the Kolmogorov-Obukhov law:

$$D \sim \lambda_e v_\lambda \sim \lambda_e(\varepsilon\lambda_e)^{1/3},$$

where ε is the mean dissipation rate, v_λ the velocity of the flow, and λ_e the mean eddy size (Monin and Yaglom, 1971, 1975). On the other hand, the temperature fluctuations which obviously are enhanced in a higher temperature environment, are also related to λ_e by

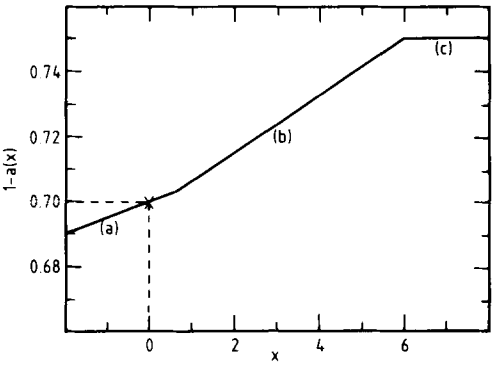

Fig. 3. Dependence of the coalbedo $1 - a(x)$ on the deviation of temperature from a reference value T_0, represented by a cross on branch (a). The slope of $1 - a(x)$ changes at branch (b) and becomes temperature independent at higher x (branch (c)).

$$T_\lambda \sim \lambda_e^{1/3}.$$

From these two relations, we conclude that in a higher temperature environment, the mean size of λ_e increases and as a result, the turbulent transport is enhanced. This should be reflected by a higher sensitivity (through the enhancement, for instance, of the hydrological cycle), a property that is well captured by a high derivative of the albedo as a function of temperature. As a matter of fact, using the results of an earlier paper (Nicolis, 1980) establishing the connection between zero-dimensional and one-dimensional climate models, we have been able to show explicitly that the albedo derivative is indeed increasing with the eddy diffusivity.

Summarizing, we can write out the explicit form of (14) as follows (note that $Q(1 - a(T_0))$ cancels with $-A$):

$$\frac{dx}{dt} = \frac{1}{C}(Q\beta_1 - B)x + \frac{1}{C}K, \quad x \leqslant x_1, \tag{15a}$$

$$\frac{dx}{dt} = \frac{1}{C}(Q\beta_2 - B)x - \frac{1}{C}Q(\beta_2 - \beta_1)x_1 + \frac{1}{C}K,$$

$$x_1 \leqslant x \leqslant x_2, \tag{15b}$$

$$\frac{dx}{dt} = -\frac{B}{C}x + \frac{1}{C}Q\beta_2 x_2 - \frac{1}{C}Q(\beta_2 - \beta_1)x_1 + \frac{1}{C}K,$$

$$x \geqslant x_2, \tag{15c}$$

where β_1, β_2 are the albedo derivatives in the two linear regions.

For a given (time-independent) value of K, eqs. (15a)–(15c) admit three steady-state solutions provided that $Q\beta_1 - B < 0$, $Q\beta_2 - B > 0$. These solutions are depicted as functions of K/C in Fig. 4. A straightforward stability analysis shows that the two extreme branches are stable, whereas the intermediate one is unstable. The lower and intermediate branch merge at a critical value of K given by

$$K^* = x_1(B - Q\beta_1), \tag{16}$$

beyond which the system is expected to perform a jump toward the upper branch.

The choice of the parameters is based on the following considerations. As these parameters fix the exact position of the two stable states, some constraints must be satisfied. For example, the present-day solution must be stable and the slope of the albedo around this state must be in agreement with the experimental or theoretical order of magnitude estimates (see, for instance, D.O.E. (1985)). Moreover according to our previous discussion in connection with climate sensitivity, in the intermediate (unstable) branch of states, β_2 must be larger than β_1. Its specific value cannot be estimated at this stage, but it must be such that the temperature jump to the upper branch of stable states has a reasonable value. The following particular set of parameters satisfies the above conditions: $\beta_1 = 5 \times 10^{-3}$, $\beta_2 = 8.7 \times 10^{-3}$, $x_1 = 0.6\ K$ and $x_2 = 6\ K$.

We now perform the following two thought experiments. First, starting from $K = 0$ (corresponding to, say, the preindustrial value of CO_2), we suddenly increase its value until the system is brought slightly above the critical point K^*, $K = K^* + \delta$. And second, we introduce a smooth linear increase of K in time, thus allowing the system to sweep the multiple steady state region until a time (the present day situation) for which K is slightly above K^*. Fig. 5 depicts the response curves $x(t)$ corresponding to these two situations. Both curves are readily obtained by a fully analytic calculation.

Let us comment successively on the two curves of Fig. 4.

(i) *Stepwise increase, Fig. 5, curve (a).* The system's temperature first increases systematically, but does not jump toward the hot climate branch, unless an induction period has elapsed. Its length, defined as the time needed to reach a value $x = 2x_1$, is given for small δ by

$$\tau_{ind} \sim \ln \frac{1}{\delta}. \tag{17}$$

This form of switching is therefore similar to the observed temperature record, whereby a systematic increase of temperature until about the middle of this century is followed by a marked slowing down (Jones et al., 1986). It highlights

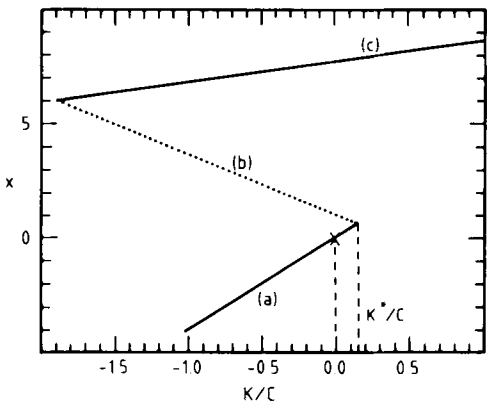

Fig. 4. Dependence of the steady state solutions of eqs. (15) on the CO_2 content K. The lower and intermediate branches merge at the critical value K^*. For the values of the parameters used, (a) and (c) are stable whereas (b) is unstable. The cross in branch (a) represents a reference state corresponding to pre-industrial climatic conditions.

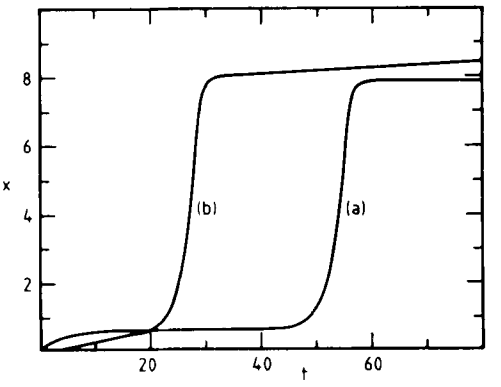

Fig. 5. Numerical integration of eqs. (15) with initial condition $x = 0$. Curve (a): sudden increase of the CO_2 content above the critical point $K = K^* + \delta$ with $\delta = 10^{-4}$. Curve (b): gradual increase, $K = \tilde{K}\varepsilon t$ with $\varepsilon = 0.01$ year^{-1} and $\tilde{K}/C = 1$ year^{-1}.

the possibility that the response to a systematic effect can be considerably delayed as a result of the system's dynamics. Let us stress that, just as in Section 2, the (possibly very large) value of heat capacity is not a satisfactory explanation of a sudden slowing down, since it affects in a similar fashion all terms contributing to the energy budget.

The inclusion of fluctuations will affect this behavior not only by introducing effects similar to those illustrated in Figs. 1 and 2, but also in two additional ways (Baras et al., 1983; Broggi et al., 1985). Firstly, the most probable value of τ_{ind} (eq. (17)) will be decreased. Secondly, and most importantly, there will be a large dispersion of the times at which the system will begin to switch to the hot climate. In other words, the overall variability will be greatly enhanced in accordance with the climatic record (Angell and Korshover, 1977).

(ii) *Gradual increase, Fig. 5, curve (b).* For $\varepsilon \ll B - Q\beta_1$ the system follows quasi-instantly the lower branch of Fig. 4b during the increase of K, till a time t^* for which K reaches the critical value K^*. It thereafter switches toward the upper branch after a very short time delay. In other words, the induction period observed for the stepwise increase of K practically disappears.

In conclusion, in the presence of multiple states, the deterministic evolution of x matches qualitatively the record only in the apparently unrealistic case of stepwise increase of CO_2. One might argue that this result is due to the fact that the three solution branches of the energy balance equation (Fig. 4) are not joined smoothly at the transition temperatures x_1 and x_2. We therefore turn, in Section 4 to the class of systems in which the lower and intermediate branch join through a differentiable curve at a value K^* of the parameter which will be referred to as *limit point* (Fig. 6). Beyond this value, the system is bound to evolve to a new branch (branch h in Fig. 6) corresponding to a hot climate.

4. Switching to the hot climate beyond a limit-point bifurcation

Another typical mode of behavior of complex systems is the limit-point bifurcation. We do not discuss in detail here the mechanisms which can give rise to a limit point, Fig. 6. Let us only quote that a limit point appears naturally if quadratic temperature dependencies are included in the albedo parameterization (Fraedrich, 1978; Wiin-Nielsen, 1984). As a matter of fact, the main interest of the analysis reported in this section is that *whatever* the details of the underlying mechanisms, the dynamics near a limit point assumes a *universal normal form* (Guckenheimer and Holmes, 1983). Choosing as before K to be zero at the reference temperature $x = 0$ ($T = T_0$) and denoting by m the value at $K = 0$ of the second (unstable) solution merging with the lower branch at the limit point, one can write the normal form (in the absence of fluctuations) as

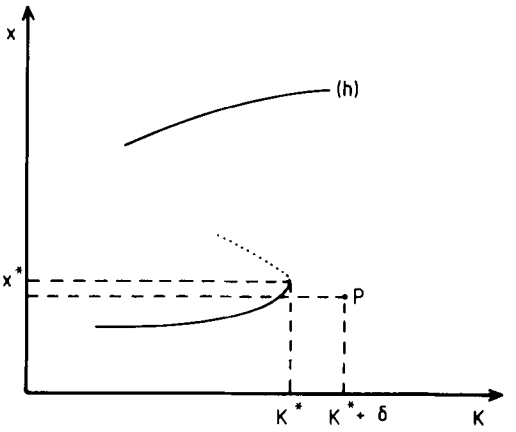

Fig. 6. Schematic representation of a limit-point bifurcation. Beyond the threshold value K^* of the control parameter, the system is bound to evolve to a new branch (h).

$$\frac{dx}{dt} = x(x - m) + K. \tag{18}$$

Let us first discard the explicit time dependence of K. The steady-state solutions of eq. (18) are then given by

$$x_{\pm} = \tfrac{1}{2}[m \pm (m^2 - 4K)^{1/2}], \tag{19a}$$

whereas the critical values of K and x at the limit point are

$$K^* = \tfrac{1}{4}m^2, \quad x^* = \tfrac{1}{2}m. \tag{19b}$$

Suppose now that the system is suddenly quenched at a state P (see Fig. 6) slightly beyond the limit point. Setting $x = x^* + \xi$, $K = K^* + \delta$, one can cast eq. (18) in the form

$$\frac{d\xi}{dt} = \xi^2 + \delta, \tag{20a}$$

whose solution is given by

$$\xi(t) = \delta^{1/2}\,\mathrm{tg}\left[\delta^{1/2}(t - t_0) + \mathrm{arctg}\,\frac{\xi_0}{\delta^{1/2}}\right]. \tag{20b}$$

This function displays a plateau (curve (a) of Fig. 7) whose length is of the order

$$\tau_{ind} \sim \frac{1}{\delta^{1/2}}, \tag{21}$$

that is to say, longer than the induction time found in the piecewise linear model (eq. (17)). Eventually x increases without bound, but this increase is of no interest here as in the real world, the system will sooner or later be attracted to the branch of states denoted by h in Fig. 6.

Let us now turn to the case of gradual increase of K. We set $K = \varepsilon t$ with $x = 0$ at $t = 0$ and ε much smaller than the inverse relaxation time along the lower branch. Proceeding as in Section 3, we then obtain curve (b) of Fig. 7, in which the aforementioned plateau has practically disappeared. Once again, we reach the conclusion that the observed temperature record is matched only in a scenario in which CO_2 would increase in a stepwise fashion.

As in the previous sections, fluctuations are likely to play an important rôle in the response. We do not discuss this point in detail, since the arguments follow exactly the same lines as before.

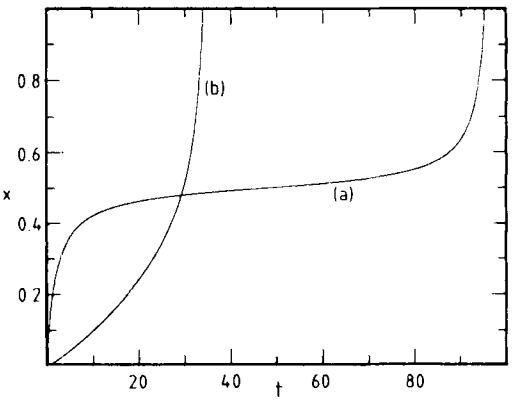

Fig. 7. Numerical integration of eq. (18) with $m = 1$ and initial condition $x = 0$. Curve (a): sudden increase of the control parameter above its critical value, $K = K^* + \delta$ with $\delta = 10^{-3}$. Curve (b): gradual increase, $K = \varepsilon t$ with $\varepsilon = 0.01$.

5. CO_2 increase and chaotic dynamics

So far, we assumed that the climatic system was perturbed relative from some pre-existing steady-state. Such a steady state may, however, be the exception rather than the rule. One of the most innovative ideas in geosciences in the last decade has been that the lack of predictability of the state of the atmosphere over a long period of time is to be attributed to the existence of *chaotic dynamics* of the key climatic variables (Lorenz, 1984). In this section, we examine the response of this type of dynamics to an increasing constraint simulating the increasing CO_2 concentration.

In studies of paleoclimatic evolution, it has been shown that non-periodic dynamics arises in a natural way when surface energy balance is coupled with the cryosphere and some external forcings (Le Treut and Ghil, 1983; Saltzman et al., 1984; Nicolis, 1987). To our knowledge, there exists no model extending this result to the short-term variability. We therefore consider as an alternative the effect of an increasing constraint on a simple model of thermal convection due to Lorenz, which produces chaotic dynamics in a certain range of parameter values (Lorenz, 1963). This model illustrates a dynamical behavior which is suggestive of some properties of the general circulation of the atmosphere. The equations are:

$$\frac{dX}{dt} = \sigma(-X + Y),$$

$$\frac{dY}{dt} = rX - Y - XZ,$$

$$\frac{dZ}{dt} = XY - bZ. \tag{22}$$

Here, X represents the lowest Fourier mode of the vertical component of convection velocity, Y and Z the lowest two Fourier modes of the temperature field, σ the Prandtl number, b a parameter related to the size of thermal convection cells, and r the reduced Rayleigh number. The latter is proportional to the vertical temperature gradient driving thermal convection. Our main assumption will be that, as a result of CO_2 increase, r increases linearly in time. We will investigate how the circulation and vertical temperature patterns will be perturbed as a result of such a time-dependent constraint.

Detailed studies of the Lorenz model (Sparrow, 1982) establish that for $\sigma = 10$ and $b = \frac{8}{3}$, the system switches from steady-state to irregular (chaotic) convection at $r_T = 24.74$. Fig. 8 gives a "standard run", indicating how one of the variables, say Y, evolves in time for a fixed $r = 26$.

We next study the behavior of the system when $r = 26 + \varepsilon t$ with $\varepsilon = 0.01$. To conform as closely as possible to the procedure followed in the monitoring of geophysical data, we construct *averages* of the variables Y (to which X is quite similar) and Z over a suitable interval of time. In the present case, a natural interval can be identified as follows. The study of the Lorenz attractor reveals that the variables undergo small-scale oscillations alternatively about the value $+(b(r-1))^{1/2}$ and $-(b(r-1))^{1/2}$, and a larger scale aperiodic motion consisting of an irregular succession of jumps between these two values.

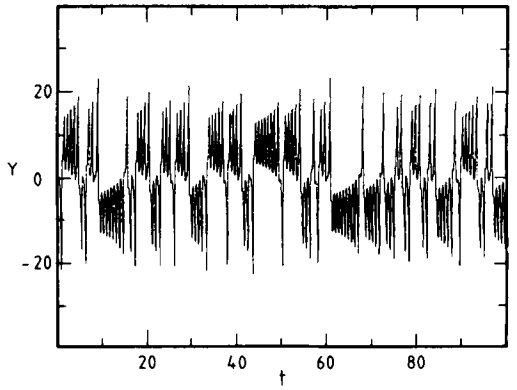

Fig. 8. Time evolution of the variable Y obtained by numerical integration of eqs. (22). Parameters used: $\sigma = 10$, $b = \frac{8}{3}$ and $r = 26$.

The pseudo-period, P, of the small-scale oscillation is given by $P = 2\pi/[b(r+\sigma)]^{1/2}$ or, for parameter values $\sigma = 10$, $b = \frac{8}{3}$ and $r = 26$, about 0.6 time units. We therefore average over a multiple nP of this period, in order to smear out the small-scale variability and focus on the principal aspects of the phenomenon, namely the large jumps. Figs. 9a, b report the behavior of the averages of the variables Y and Z. We see that Y hardly perceives the increase of constraint, whereas in contrast, Z follows it in a rather straightforward manner. This result shows how subtle the response of a complex system to a parameter may be (see also Erneux and Mandel, 1986). Depending on the monitored variable, the system may look insensitive (Fig. 9a) or sensitive ((Fig. 9b) to the parameter over a substantial period of time, which in the figure runs up to about 500 time units. Following this limit, however, a further increase of r may change the qualitative features of the dynamics by bringing the system to a new attractor.

Figs. 10a, b depict the time evolution of the variances of the Y and Z variables around the above-defined means. We see that both variances exhibit a systematic increasing trend. This suggests the interesting possibility that the monitoring of a similar quantity for the surface temperature may reveal a clearer trend toward increased CO_2 concentration than the more ambiguous trend of the mean.

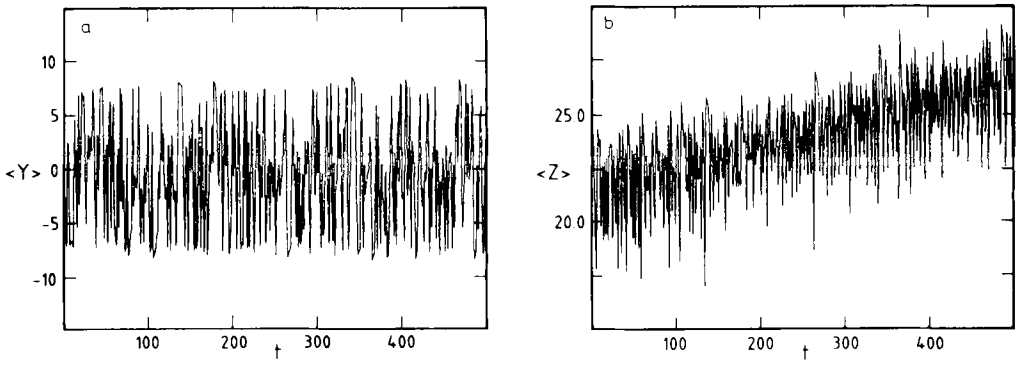

Fig. 9. The evolution of averages of the variables Y (a) and Z (b) over twice the pseudo-period of the system. Parameters as in Fig. 8 but $r = 26 + \varepsilon t$ with $\varepsilon = 0.01$.

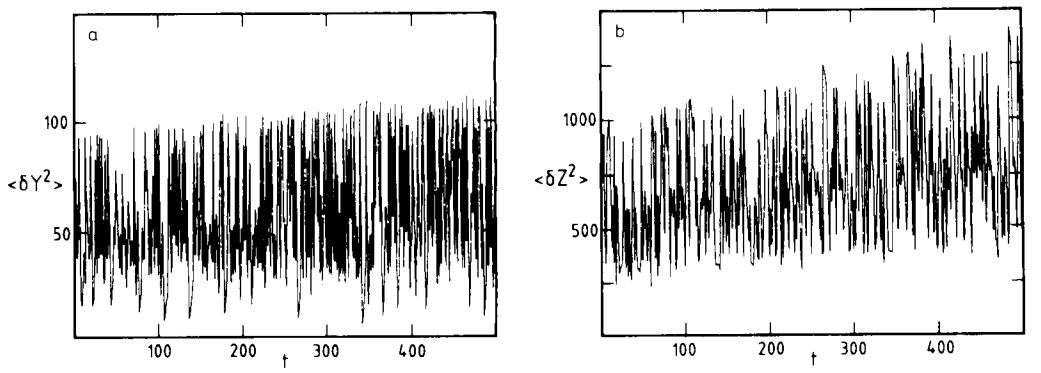

Fig. 10. Time evolution of the variance of the variables Y (a) and Z (b) around the averages of Fig. 9.

Let us outline a qualitative explanation of the insensitivity of the means of X and Y. The amplitude of the small-scale oscillations over which we have averaged in Fig. 9 is given in a first approximation by $r^{1/2}$. If r varies on a slow time scale compared to the above pseudo-period, the averaging of the variable over the pseudo-period will practically eliminate the oscillation and thus also the r dependence of its amplitude. Meanwhile, since the large-scale jumps take place between states which have identical dependencies on r, an increase of r over time will not affect the overall pattern of time-dependence of the variable. The situation is different for the variance, since the square of an oscillating variable averaged over a time close to the period gives a non-vanishing contribution, here essentially proportional to $r(t)$. Thus, the variance is bound to depend on t in a way similar to the constraint, in agreement with our numerical results. Incidentally, this argument can be applied with practically no modification to the response of a limit cycle oscillation close to a Hopf bifurcation, to a systematic increase of the bifurcation parameter.

6. Concluding remarks

We have seen that a dynamical system subjected to a systematic increase of a control parameter need not produce a response following this increase in a passive manner. Depending on the phenomenon and on the variable that is monitored, stages of marked slowing down can be observed, or even a situation in which the variable shows no increasing trend whatsoever.

One mechanism giving rise to slowing down reminiscent of the record, is the action of stochastic perturbations, especially those having a relatively long correlation time. We believe that such perturbations are especially adequate to account for the interaction between atmospheric dynamics and the oceans. A second mechanism of great generality is sudden switching in the vicinity of a point of marginal stability. At first sight, it seems that this mechanism cannot be related to present-day increase of CO_2, whose time scale is long compared to the characteristic relaxation time of the mixed layer. Still, it may account for past episodes of CO_2 release from natural causes, or for the response to perturbations related to an increase of other trace gas concentrations. A third mechanism that has been identified is oscillatory dynamics. We explored this dynamics in the chaotic region since, to our knowledge, there is no indication in the literature of endogenous periodic behavior in short-term climatic variability.

A surprising result of our analysis is that while the mean of a variable may hardly perceive the systematic CO_2 increase, the variance may be very sensitive to it. This suggests the interesting possibility that the monitoring of the variance of global surface temperature may provide us with a useful, very sensitive index for forecasting systematic trends.

The ideas developed in the present paper were implimented on very simple climate models. It

should undoubtedly be interesting to follow a similar procedure using more detailed energy balance and global circulation models, in which the parameters reflecting the effect of CO_2 can be identified in a more quantitative manner.

7. Acknowledgements

This work is supported, in part, by the European Economic Community under contract no. ST2J-0079-1-B(EDB).

REFERENCES

Angell, J. K. and Korshover, J. 1977. Estimate of the global change in temperature surface to 100 mb, between 1958 and 1975. *Mon. Wea. Rev. 105*, 375–385.

Augustsson, T. and Ramanathan, V. 1977. A radiative convective model study of the CO_2 climate problem. *J. Atmos. Sci. 34*, 448–451.

Baras, F., Nicolis, G., Malek-Mansour, M. and Turner, J. W. 1983. Stochastic theory of adiabatic explosion. *J. Stat. Phys. 32*, 1–23.

Broecker, W. S. 1975. Climatic change: Are we on the brink of a pronounced global warming? *Science 189*, 460–463.

Broggi, Lugiato, L. A. and Colombo, A. 1985. Transient bimodality in optically bistable systems. *Phys. Rev. 32A*, 2803–2812.

Bryson, R. A. and Dittberner, G. J. 1976. A non-equilibrium model of sea surface temperature. *J. Atmos. Sci. 33*, 2094–2106.

D.O.E./ER-0237, 1985. *Projecting the climatic effects of increasing carbon dioxide*. US Department of Energy, Washington, DC.

Erneux, T. and Mandel, P. 1986. Imperfect bifurcation with a slowly-varying control parameter. *SIAM J. Appl. Math. 46*, 1–15.

Fraedrich, K. 1978. Structural and stochastic analysis of a zero-dimensional climate system. *Q. J. R. Meteorol. Soc. 104*, 461–474.

Gardiner, C. W. 1983. *Handbook of stochastic methods*. Springer, Berlin.

Guckenheimer, J. and Holmes, P. 1983. *Nonlinear oscillations, dynamical systems and bifurcations of vector fields*. Springer, Berlin.

Hoffert, M. I., Callegari, A. J. and Hsieh, C. T. 1980. The role of deep sea heat storage in the secular response to climatic forcing. *J. Geophys. Res. 85*, 6667–6679.

Hoffert, M. I. and Flannery, B. P. 1985. Model projections of the time dependent response to increasing carbon dioxide. In: *Projecting the climatic effects of increasing carbon dioxide*, Report D.O.E./ER-0237. US Department of Energy, Washington, DC, 151–190.

Idso, S. B. 1982. *Carbon dioxide—Friend or Foe?* IBR press, Tempe, Arizona.

Jones, P. D., Wigley, T. M. L. and Wright, P. B. 1986. Global temperature variations between 1861 and 1984. *Nature 322*, 430–434.

Keeling, C. D. and Bacastow 1977. Impact of industrial gases on climate. In: *Energy and climate*, Geophysics Study Committee, National Academy of Sciences, Washington, DC, 72–95.

Le Treut, H. and Ghil, M. 1983. Orbital forcings, climatic interactions and glaciation cycles. *J. Geophys. Res. 88*, 5167–5190.

Lorenz, E. N. 1963. Deterministic nonperiodic flow. *J. Atmos. Sci. 20*, 130–141.

Lorenz, E. N. 1984. Irregularity: a fundamental property of the atmosphere. *Tellus 36A*, 98–110.

Monin, A. S. and Yaglom, A. M. 1971. *Statistical fluid mechanics*, vol. I, M.I.T. Press, Cambridge.

Monin, A. S. and Yaglom, A. M. 1975. *Statistical fluid mechanics*, vol. II, M.I.T. Press, Cambridge.

Newell, R. E. and Dopplick, T. G. 1979. Questions concerning the possible influence of anthropogenic CO_2 on atmospheric temperature. *J. Appl. Meteorol. 20*, 114–117.

Nicolis, C. 1980. Derivation of zero-dimensional from one-dimensional climate models. *J. Geophys. Astrophys. Fluid Dyn. 14*, 91–103.

Nicolis, C. and Nicolis, G. 1981. Stochastic aspects of climatic transitions—Additive fluctuations. *Tellus 33*, 225–234.

Nicolis, C. 1987. Long-term climatic variability and chaotic dynamics. *Tellus 39A*, 1–9.

Saltzman, B., Hansen, A. R. and Maasch, K. A. 1984. The late quaternary glaciations as a response of a three-component feedback system to earth-orbital forcing. *J. Atmos. Sci. 41*, 3380–3389.

Schneider, S. H. and Mass, C. 1975. Volcanic dust, sunspots and temperature trends. *Science 190*, 741–746.

Sparrow, C. 1982. *The Lorenz equations*. Springer, Berlin.

Wiin-Nielsen, A. 1984. On simple climate models with periodic and stochastic forcing. *Geoph. Astrophys. Fluid Dyn. 28*, 1–30.